Physica Scripta

An International Journal for Experimental and Theoretical Physics

Dear Author,

Please find attached a PDF of your article that has appeared in issue T114 of Physica Scripta. This file has been optimised for viewing on screen, but can be printed off. If you would like a version of this file, optimised for printing, or would like to purchase a number of printed copies of your paper, please contact me.

Best Wishes,

Christine Shaw
Journal Controller
Marston Digital
Omega Park
Collet
Didcot
OX11 7AW
email: shawc@lrl.com
voice: +44 1235 518700
fax: +44 1235 515777
web: http://www.physica.org

Editorial office	Telephone	Electronic Mail	Home Page
Physica Scripta **The Royal Swedish Academy of Sciences** **Box 50005** **S-104 05 Stockholm, Sweden**	+46-(0)8-673 95 00	physica@kva.se	http://www.physica.org

Physica Scripta. Vol. T114, 44–48, 2004

Finite-Temperature Effects on Correlation of Electrons in Quantum Dots

Markku Leino and Tapio T. Rantala*

Institute of Physics, Tampere University of Technology, P.O. Box 692, FIN-33101 Tampere, Finland

Received September 2, 2003; accepted October 22, 2003

PACS number: 73.21.La

Abstract

The path-integral Monte Carlo method is used to examine the two-electron state of a model quantum dot. Electrons in the two-dimensional quantum dot are confined by a harmonic oscillator potential of strength $\hbar\omega = 1$ eV. Mixed state densities, energies and pair correlation functions are evaluated at various temperatures, and their temperature dependencies are analyzed. Also, the two-electron pure state energetics is resolved and the correlation induced shifts of the first and second excited states are evaluated.

1. Introduction

Quantum dots are small man-made structures in a solid, typically with sizes ranging from nanometers to a few micrometers. They consist of 10^3–10^9 atoms with an equivalent number of bound electrons. Electrons are tightly bound to the atomic cores and bonds except for a small fraction of free charge carriers [1]. Current nanofabrication technology allows precise control of the size and shape of these dots. Thus, the size and shape of the confining potential and the effective mass of charge carriers can be adjusted to tune the electronic structure and the excitation spectrum, in particular [2].

Properties of few-electron quantum dots, e.g. at heterojunction interfaces, are important to understand for the development of novel semiconductor technology. In semiconductor laser technology, quantum dots may provide unique opportunities in developments and advance the applications [3]. Thus, the quantum dots are convenient for optoelectronic device design and fascinating for theoretical studies. From the theoretical point of view the quantum dots are atomic-like systems with localized electronic states. Thus, atomic physics can be applied here to the field of semiconductor devices.

The two-electron system is one of the simplest non-trivial quantum mechanical systems. Nevertheless, some analytical results exist for two electrons in a symmetrical enough quantum dot. Taut [4] reduced the problem of solving a six-dimensional partial differential equation to finding the real roots of a polynomial, and thus, gave analytic solutions to particular oscillator frequencies of two interacting electrons in an external harmonic oscillator potential. Dineykhan and Nazmitdinov [5] found analytic expressions for the ground state energy for 2D and 3D harmonic oscillators in external magnetic fields.

In addition to analytical results, there are a number of numerical results for two-electron quantum dots. A numerically exact calculation for the energy spectra of two electrons in a finite height cylindrical quantum dot by a coupled-channel method is presented in details by Lin and Jiang [6]. Harju *et al.* [7] studied the ground state of parabolically confined electrons in a quantum dot by both direct numerical diagonalization and variational Quantum Monte Carlo methods. In an older paper Harju *et al.* [8] applied the Quantum Monte Carlo technique to a two-electron quantum dot. Merkt, Huser and Wagner [9] have calculated the discrete energy spectra for two electrons in a two-dimensional harmonic well in the effective-mass approximation as a function of the dot size and the strength of a magnetic field directed perpendicular to the dot plane using first order perturbation theory. Furthermore, the states of two-electron paired quantum well quantum dots [10] were calculated with diagonalization and the variational principle.

More complicated quantumd dots have been studied by many methods: Perturbation theory [11], numerical diagonalization [12], density-functional theory [13, 14], unrestricted Hartree-Fock [15], diffusion Monte Carlo [16] and path-integral Monte Carlo [17, 18, 19, 20, 21, 22, 23] methods. In these studies electronic structure, addition spectra, electronic states, Fermi liquid and Wigner molecule behaviour, ground and excited state energies, shell effects, electron correlations and low-energy states were examined.

Even for the correlation energy in a quantum dot a simple but accurate analytic expression can be found in Wentzel–Kramers–Brilloun approximation [24]. The behavior of 3D exchange–correlation energy functional approximation of DFT in anisotropic systems with 2D character is investigated by Kim *et al.* [25]. They pointed out a fundamental limitation of LDA, due to the nonlocal nature of exchange–correlation hole.

The physics of interactions becomes especially interesting in zero external magnetic field, when electron spins are not polarized and are active players in the game [26].

In this study, we apply the path-integral Monte Carlo simulation method [27] to investigate the properties of a two-electron quantum dot. We evaluate the one-electron distributions and two-electron correlation functions, and temperature effects on both. Furthermore, we resolve the finite-temperature mixed states to the contributing pure states, and by that, we are able to consider the transition energies, and thus, the optical response of charge carriers. Also, the correlation effect on transition energies is discussed.

In the next chapter we briefly review the theoretical concepts of Monte Carlo methods and the optimization algorithm needed here. Then, in chapter 3 we give the simulation results and compare those to the analytical one-electron results. Chapter 4 is devoted to the case of two correlated electrons, and conclusions are given in chapter 5.

2. Method

In this chapter we briefly describe the basic concepts of PIMC method, the Monte Carlo simulation procedure we used and the

*email: Tapio.Rantala@tut.fi

© *Physica Scripta 2004*

optimization scheme that was used to resolve the pure many-body eigenstates from the mixed state.

2.1. *Path-Integral Monte Carlo method*

All stationary properties of a d-dimensional quantum N-body system with Hamiltonian $\widehat{H} = \widehat{T} + \widehat{V}$ in thermal equilibrium at temperature $\beta \equiv 1/k_B T$ are obtained from the density matrix $Z = \mathrm{Tr}\, \mathrm{e}^{\beta \widehat{H}}$ [28]. Here, $\widehat{T} = \sum_{i=1}^{N} \widehat{\boldsymbol{p}}_i^2/2m_i$ is the kinetic energy operator and $\widehat{V}$ includes the external potential and interactions between particles.

2.1.1. *Path-Integral Formalism.* In discrete path-integral representation the density matrix is

$$Z = \left(\frac{mM}{2\pi\hbar^2\beta}\right)^{dN/2} \int \exp\left[-\beta \sum_{n=1}^{M} (K_n + U_n)\right] \mathrm{d}\boldsymbol{r}_0 \cdots \mathrm{d}\boldsymbol{r}_{M-1}, \tag{1}$$

where operators K_n and U_n define internal and external energies of the system. In the primitive approximation [27] they are written as

$$K_n = \frac{mM}{2\hbar^2\beta^2}(\boldsymbol{r}_{n-1} - \boldsymbol{r}_n)^2, \tag{2a}$$

$$U_n = \frac{1}{2M}(V(\boldsymbol{r}_{n-1}) + V(\boldsymbol{r}_n)), \tag{2b}$$

where m is the effective mass of the electrons and M is called the Trotter number, and $\boldsymbol{r}_0 = \boldsymbol{r}_M$. The primitive approximation, where the external energy coincides with potential energy, contains all the physics and converges to the correct limit, given a small enough β/M [27]. Furthermore, it is simple and well defined, and at the limit $M \to \infty$ the true many-body description (1) is exact.

It is straightforward to calculate scalar operators, such as density, potential energy, and the pair correlation functions; they are simply averages over the paths [27]. Use can be made of the symmetry in imaginary time, since all time slices t are equivalent. Thus, the average density and pair correlation functions are

$$\rho(\boldsymbol{r}) = N_\rho \sum_{n,t} \langle \delta(\boldsymbol{r} - \boldsymbol{r}_{nt}) \rangle \tag{3a}$$

and

$$g(\boldsymbol{r}) = N_g \sum_{n,i,j,t} \langle \delta(\boldsymbol{r} - (\boldsymbol{r}_{nit} - \boldsymbol{r}_{njt})) \rangle, \tag{3b}$$

where N_ρ and N_g are proper normalization factors, i and j refer to different particles, and n and t are as above.

The nondiagonal properties in coordinate basis, such as the energy, free energy, and momentum distribution, are not so straightforward to calculate. A thermodynamic estimate of the energy is obtained by differentiating the partition function with respect to the inverse temperature [27] as

$$E(\beta) = -\frac{1}{Z}\frac{\mathrm{d}Z}{\mathrm{d}\beta} = M\langle dN/(2\beta) - K_n + U_n/M \rangle. \tag{4}$$

Path-integral Monte Carlo (PIMC) simulation method is a "numerically exact" finite-temperature approach, the only limiting factor being computational capacity, for evaluation of the density matrix (1).

2.1.2. *Monte Carlo simulation procedure.* The quantum-mechanical approximation of the finite temperature density matrix of the N-particle system, Eq (1), is a multidimensional integral [29, 28], which turns out to be a partition function of a classical $M \times N$-particle canonical ensemble or NVT-system. This specific classical system consists of N closed chains or "polymers" of M knots or "beads" in a necklace with a certain special description of interactions among the particles and between the external potential. Thus, quantum-mechanical density matrix can be evaluated using classical formalism.

We use the Metropolis Monte Carlo scheme to evaluate the integral (1). With this technique all the approximations in integration scheme and in path-integral formulation are controllable. The Metropolis algorithm samples very effectively the correct distribution of beads and thus the correct density matrix Z using the integrand in (1) as the weight for the importance sampling process. The main issue is whether the configuration space is explored thoroughly in a reasonable amount of computer time. Including many types of Monte Carlo moves makes the algorithm more robust, since before doing a calculation one does not necessarily know which type of moves will lead to a balanced sampling of the phase space and rapid convergence of expectation values. We used two types of moves: one randomly selected bead in one random necklace and the center of mass of a random necklace.

Distribution of steps in the phase space was taken to be Gaussian such that the total Metropolis acceptance rate is about 70% and the frequency of each move is about the same. This is called the *classic rule* [27].

2.2. *Finding the pure states*

The density matrix (1) is a finite temperature, mixed state, description of the quantum system. Thus, the mixed state energy $E(\beta)$ at temperature T, Eq (4), is the Boltzmann weighted mean value of pure state eigenenergies E_i

$$E(\beta) = \frac{\sum_i d_i E_i \mathrm{e}^{-\beta E_i}}{\sum_i d_i \mathrm{e}^{-\beta E_i}}, \tag{5}$$

where the summation is done over all states i weighted by the degeneracy d_i. In principle, the contribution of excited state energies E_i can be separated from equation (5) by fitting, if the function $E(\beta)$, Eq (4), is known analytically or can be simulated accurately enough. In finding the pure states, the infinite summation (5) is approximated by a function $f(\beta, \boldsymbol{E}) = \sum_{i=0}^{m} d_i E_i \exp(-\beta E_i) / \sum_{i=0}^{m} d_i \exp(-\beta E_i)$, where $\boldsymbol{E}$ is a finite (truncated) vector containing the pure state energies E_i, $i = 0, 1, \ldots, m$. In principle, it should be possible to find the pure state densities $\rho_i(\boldsymbol{r})$ independently with the same procedure, and thus, find a verification of pure state energies E_i obtained here.

From simulations at various temperatures T_j we sampled the mean energy function, and found it very similar to the one-electron mixed state energy function, see below. The differences in ground state energy E_0 and scaling with respect to β were determined. We found the excited state eigenenergies E_i by fitting the energy formula (5) in the least squares sense. Two optimization methods for fitting were tested, Gauss–Newton and Levenberg–Marquardt algorithms [30, 31]. Both use quadratic approximations to nonlinear residual vector, but L–M is so called trusted region algorithm, i.e., it moves only in the region where the fit is good, discarding too long steps.

Actually, the Gauss–Newton method was not good enough. It is possible to find a few first pure states with that method,

but Levenberq–Marquardt was much simpler to use and more eigenenergies were found, and the algorithm is almost as simple.

The optimization can be simplified because of Boltzmann distribution: at low enough temperature we get only one or two states that contribute to the total energy. Thus, we can find easily a few lowest eigenenergies and when purifying more states, the lowest states can be fixed.

One should note that the high temperature here is a computational tool, only, and has nothing to do with any realistic temperature related to quantum dots.

3. Single electron case

The one-electron harmonic oscillator is analytically solvable in any dimensions. The eigenenergies of the 2D harmonic oscillator are $E_i = \hbar\omega(1 + i)$, where $i = 0, 1, \ldots$. The degeneracy d_i of the state i is $i + 1$ for a 2D harmonic oscillator. The same degeneracy is assumed for the two-electron case. When all states weighted by the respective Boltzmannian probality are summed, Eq (5), we get the temperature dependent energy [28] per dimension

$$\langle E\rangle = \frac{\hbar\omega}{2}\coth\frac{\hbar\omega\beta}{2}, \tag{6}$$

which explicitly shows how the temperature and the confining potential are related. Similarly, the electron densities of pure states can be summed up to give the temperature dependent density and by convolution we obtain the pair correlation function for the non-interacting particles.

Thus, we can test the path-integral Monte Carlo code and optimization methods for the single electron case with analytical energies and electron densities. Both methods turned out to work fine. In figure 1, the one-electron states (energies, wavefunctions, occupations and probabilities) are demonstrated. Note that this one-electron energy diagram is identical with the excited states diagram of the non-interacting N-electron quantum dot.

The L–M algorithm is stable with respect to changes in starting point and temperature in the one-electron case. Thus, the pure one-electron eigenstates E_i can be found until $i \approx 7$ easily, if replacing simulated (4) by the analytical formula (6) in fitting. However, the optimization is sensitive to the accuracy in mixed state energy: if the analytical energies are rounded to two decimals, the fitting procedure does not work reliably.

4. Two-electron correlations

The system we consider is two Coulomb-interacting opposite spin electrons in a two-dimensional quantum dot. The lateral confinement is approximated by a harmonic potential assuming circular symmetry and "strength" $\hbar\omega = 1$ eV. Thus, the confinement is very strong corresponding to a QD of a few nanometers and a few hundreds atoms, only. This serves, however, as a nice model and may be realistic with new fabrication technologies. Assuming GaAs as the material we use the electron effective mass $m = 0.067m_e$ and the dielectric constant $\epsilon = 12.4$.

The two-electron case with Coulomb interaction looses the full separability, and the Hamiltonian can be reduced to center-of-mass and relative motion, only. The wave function for the center-of-mass can be solved analytically, but that describing the relative motion must be solved using numerical methods. With the PIMC method we treat the full Hamiltonian numerically, too.

4.1. *Distributions*

In fig 2 we compare the one-electron densities of the non-interacting or the single electron case to the case of two interacting electrons, at two different temperatures. In the upper panel we see the temperature broadening clearly but hardly any correlation effects. However, the difference curves in the lower panel reveal the weak modifications due to the Coulomb repulsion, which tends to keep the electrons apart from each other. The resulting balance seems to be: one at the center of QD and the other away, rather than both slightly off from the center. Surprisingly, the difference is larger at the higher temperature. We do not expect Wigner crystallization type of electron localization in our case, because the effective density parameter here is $r_s^* \approx 0.15$, the threshold being $r_s \geq 7.5$ [32].

Figure 3 shows the pair correlation functions for these two cases together with the corresponding non-interacting case Gaussian reference function. Changes in pair correlation functions due to the Coulomb interactions are illustrated in Fig 4. In addition to temperature broadening the correlation effects are clearly seen,

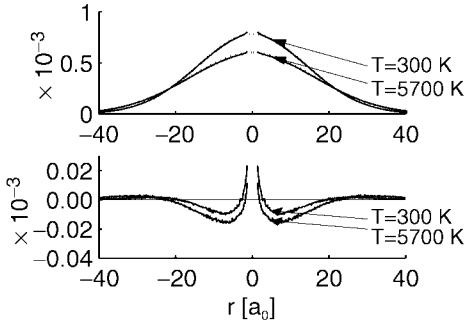

Fig. 2. One-electron densities for non-interacting or single- (dashed) and two-electron (solid) systems, upper panel. Also, the differences of correlated and non-interacting case densities are shown in the lower panel (r in atomic units, $a_0 \approx 0.52$ Å).

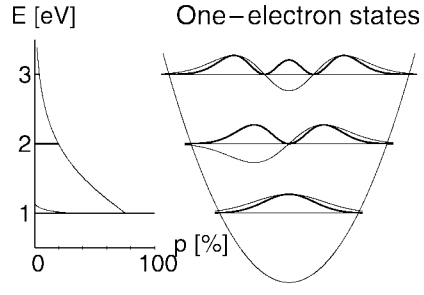

Fig. 1. One-electron states for the 2D harmonic oscillator with $\hbar\omega = 1$ eV. The energy levels, with wavefunctions, densities and probabilities are shown with Boltzmann distribution for $T = 300$ K and $T = 5700$ K.

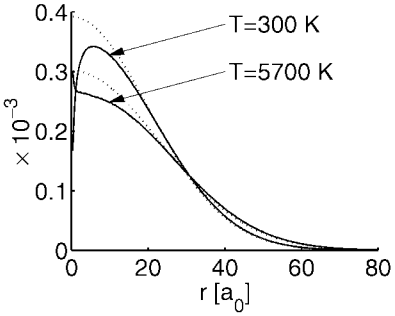

Fig. 3. Pair correlation functions $g(r)$ of the two interacting electrons. Normalization with weight $2\pi r$ is adjusted to unity.

© *Physica Scripta 2004*

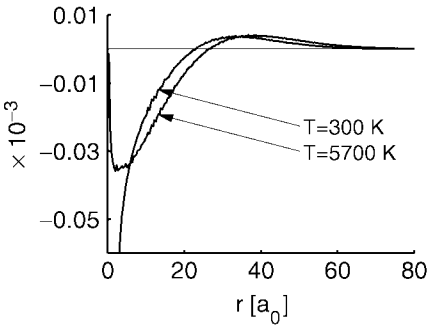

Fig. 4. Difference of pair correlation functions of the interacting and non-interacting electrons, evaluated from the functions in Fig 3.

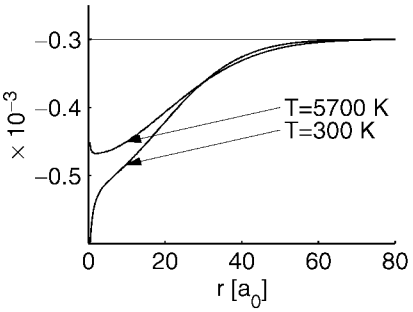

Fig. 5. The average Coulomb correlation hole. Normalization to unity with the weight factor $2\pi r$.

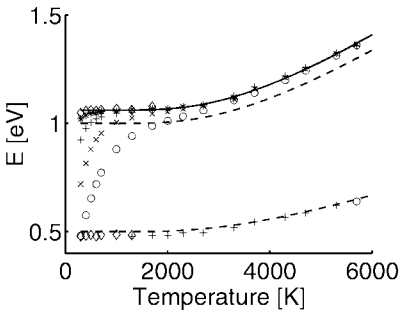

Fig. 6. Mixed state energy as a function of temperature of the correlated two-electron system, simulated with Trotter numbers 8 (○), 16 (×), 32 (+), 64 (∗) and 128 (◇) Solid line is a fit with functional form (6) and dashed lines show analytical single electron total and kinetic (potential) energies, respectively. The high temperatures are only a computational tool to make the resolution of the mixed state to pure states and, of course, have nothing to do with any realistic temperatures of any QDs.

too. The short range repulsive correlation (at a few a.u.) is strong at room temperature, whereas it becomes weaker further away (from 10 a.u.), as compared to the 5700 K case. At the $r \to \infty$ limit the behavior is remarkably different. That however, may not be relevant in any real 2D system, where the third dimension is inevitably present.

We define the average correlation hole as $g(r) - 2g_1(r)$ where $g_1(r)$ is the non-interacting case (Gaussian shaped) pair correlation function. This is shown in Fig 5. It supports the conclusions above, except for the range: the room temperature repulsive Coulomb correlation hole is more pronounced, as expected.

4.2. *Excitation energetics*

The analytical average energy of the single electron mixed state as a function of T, Eq (6), is shown in Fig 6. Also the equal contributions from the kinetic and potential energies are shown. The low temperature limit is 1 eV (0.5 eV) and contributions from lowest excitation appear just below 2000 K.

The simulated interacting case energies are shown for different Trotter numbers $M = 8, \ldots, 128$ and temperatures. The asymptotic low temperature limit should be similar to the single-electron case: contribution from the ground state, only. It is nicely seen how the small M energies deviate from this at low T, thus failing in describing the quantum (kinetic) energy. However, from low-T fitting the ground state energy 1.06 eV is found. Contributions from kinetic, external and Coulomb repulsion are 0.48 eV, 0.52 eV and 0.06 eV, respectively.

The Coulomb interaction keeps the electrons more apart than the noninteracting counterparts, which decreases the kinetic energy but increases potential energy [25]. In Fig 6, it can be seen that the kinetic energy decreases some 0.02 eV at low temperature, that is, in quantum regime, but the effect becomes smaller with increasing temperature.

The high-T behavior is seen to be similar to the single electron case, though the analytical form (6) probably cannot be assumed. However, a fit to (6) results in a scaling factor 0.48 for β.

Resolution of the excited states by fitting $f(\beta, \boldsymbol{E})$ to simulated $\{E(\beta_j)\}$, as described above, leads to the two first excited energies 1.00 eV and 1.9 eV above the ground state. Thus, the correlation has an equal effect on the two lowest state energies but less on the third, the second excited state. This probably can be related to decreasing Coulomb energy with increasing excitation energy.

As a QD becomes larger, the energy difference between single-particle quantum states in the QD becomes smaller and the single-particle quantum states can mix thoroughly to construct many-body quantum states at low-T, already. In general, many-body quantum states are determined by competition between single-particle energy spacing and Coulomb interaction [33, 25, 10].

5. Conclusions

We have shown that the path-integral Monte Carlo method is suitable for the study of two-dimensional two-electron quantum dot. The temperature effects and role of electron-electron correlations, in particular, are nicely demonstrated.

An expected temperature broadening of one-electron distribution was found. However, a detailed inspection of correlations in terms of pair correlation functions and correlation hole reveales differences in the nature of correlation in two different temperatures.

It is also demonstrated how (unreasonably) high temperature simulations and the resulting mixed state data can be used to resolve the pure quantum state properties. This was applied here to determine the excited state energetics, but the related densities or wavefunctions could be found similarly. In the present case, two-dimensional quantum dot with harmonic ($\hbar\omega = 1$ eV) confining potential, the two lowest two-electron states shift by 0.06 eV, 0.06 eV up and the third 0.1 eV down in energy as a result from electron-electron Coulomb correlation.

References

1. Kouwenhoven, L., Austing, D. and Tarucha, S., Rep. Prog. Phys. **64**, 701 (2001).
2. Reimann, S. M. and Manninen, M., Rev. Mod. Phys. **74**, 1283 (2002).
3. Ledentsov, N. N., Grundmann, M., Heinrichsdorff, F. and Bimberg, D., IEEE J. Selected Topics Quant. Electron. **6**, 439 (2000).
4. Taut, M., Phys. Rev. A. **48**, 3561 (1993).

© *Physica Scripta 2004*

5. Dineykhan, M. and Nazmitdinov, R., Phys. Rev. B **55**, 13707 (1997).
6. Lin, J. T. and Jiang, T. F., Phys. Rev. B **64**, 195323 (2001).
7. Harju, A., Sverdlov, V. and Nieminen, R., Phys. Rev. B **59**, 5622 (1999).
8. Harju, A., Sverdlov, V., Barbiellini, B. and Nieminen, R., Physica B **255**, 145 (1998).
9. Merkt, U., Huser, J. and Wagner, M., Phys. Rev. B **43**, 7320 (1991).
10. Ugajin, R., Suzuki, T., Nomoto, K. and Hase, I., J. Appl. Phys. **76**, 1041 (1994).
11. Rontani, M., Rossi, F., Manghi, F. and Molinari, E., APL **72**, 957 (1998).
12. Ezaki, T., Mori, N. and Hamaguchi, C., Phys. Rev. B **56**, 6428 (1997).
13. Lee, I.-H., Rao, V., Martin, R. M. and Leburton, J.-P., Phys. Rev. B **57**, 9035 (1998).
14. Hirose, K. and Wingreen, N. S., Phys. Rev. B **59**, 4604 (1999).
15. Reusch, B., Häusler, W. and Grabert, H., Phys. Rev. B **63**, 113313 (2001).
16. Pederiva, F., Umrigar, C. J. and Lipparini, E., Phys. Rev. B **62**, 8120 (2000).
17. Harting, J., Mülken, O. and Borrman, P., Phys. Rev. B **62**, 10207 (2000).
18. Häusler, W., Reusch, B., Egger, R. and Grabert, H., Physica B **284**, 1772 (2000).
19. Mak, C., Egger, R. and Weber-Gottschick, H., Phys. Rev. Lett. **81**, 4533 (1998).
20. Egger, R., Häusler, W., Mak, C. and Grabert, H., Phys. Rev. Lett. **82**, 3320 (1999).
21. Dikovsky, M. V. and Mak, C. H., Phys. Rev. B **63**, 235105 (2001).
22. Sundqvist, P. A., Volkov, S. Y., Lozovik, Y. E. and Willander, M., Phys. Rev. B **66**, 075335 (2002).
23. Lozovik, Y. E., Volkov, S. Y. and Willander, M., Solid State Commun. **125**, 127 (2003).
24. García-Castelán, R. M. G., Choe, W. S. and Lee, Y. C., Phys. Rev. B **57**, 9792 (1998).
25. Kim, Y.-H. *et al.*, Phys. Rev. B **61**, 5202 (2000).
26. Mikhailov, S. A., Phys. Rev. B **66**, 153313 (2002).
27. Ceperley, D. M., Rev. Mod. Phys. **67**, 279 (1995).
28. Feynman, R. P., "Statistical Mechanics" (Addison Wesley, 1972, 1988).
29. Feynman, R. P. and Hibbs, A. R., "Quantum Mechanics and Path Integrals" (New York: McGraw-Hill, 1965).
30. Fletcher, R., "Practical methods of optimization" (John Wiley & Sons Ltd, 1978).
31. Nash, S. G. and Sofer, A., "Linear and Nonlinear Programming" (MacGraw-Hill, 1996).
32. Chui, S. T. and Tanatar, B., Phys. Rev. Lett. **74**, 458 (1995).
33. Bryant, G. W., Phys. Rev. Lett. **59**, 1140 (1987).

© *Physica Scripta 2004*